J. Exp. Biol. (1970), **52**, 345–367
With 18 *text-figures*
Printed in Great Britain

AERODYNAMICS OF GLIDING FLIGHT IN A FALCON AND OTHER BIRDS

BY VANCE A. TUCKER AND G. CHRISTIAN PARROTT
Department of Zoology, Duke University, Durham, North Carolina

(*Received* 26 *September* 1969)

INTRODUCTION

An interesting characteristic of avian gliders is their ability to soar or remain aloft without flapping their wings for long periods. There are two ways to do this. In static soaring a bird maintains or gains altitude by gliding in air that has an upward velocity component equal to or greater than the bird's sinking speed. In dynamic soaring a bird uses changes in the horizontal wind-velocity component to stay aloft, and no upward wind component is required. The ability of a bird to use either method depends on its aerodynamic characteristics and on atmospheric conditions.

The aerodynamic characteristics of a gliding aircraft such as a bird can be determined from gliding performance, which includes a description of the glide path of the aircraft flying at constant speed through still air. This description may be obtained from direct measurements. Alternatively, gliding performance can be determined from aerodynamic characteristics, which usually are measured in a wind tunnel by mounting an aircraft, a model of it, or pieces of it, on a flight balance.

Both sorts of measurements have been difficult to make on birds. Several estimates of gliding performance based on observations in nature have been published, but these do not have sufficient accuracy for aerodynamic purposes. Aerodynamic force measurements on stuffed, frozen, or sculptured models mounted in wind tunnels are questionable because the shapes and surface features of the models may deviate significantly from those of their living counterparts. Catalogued aerodynamic information used by aircraft designers is usually not applicable to birds because of the disparity in speed and size between birds and man-made aircraft.

The gliding performance of a living bird may be measured accurately if the bird is trained to glide freely in a wind tunnel that can tilt along its longitudinal axis. By altering the tilt of the tunnel and the speed of air flow, one can reproduce the aerodynamic and gravitational forces that act on a bird gliding at various speeds in nature. This method has been used for the pigeon (*Columba livia*; Pennycuick, 1968), and we have used it to investigate the gliding performance of a laggar falcon (*Falco jugger*). Laggar falcons are native to India and are similar to the more familiar peregrine falcon (*F. peregrinus*) in size and proportions. Although falcons are usually thought of as active fliers, they also glide and soar (Beebe & Webster, 1964).

AERODYNAMIC RELATIONS

Aerodynamic forces are described in the conventional manner as lift (L) and drag (D), which are respectively perpendicular and parallel to the bird's path through

the air. This study confines itself to gliding flight without acceleration (equilibrium gliding), and in this condition the lift and drag forces are balanced by weight (W) components (Fig. 1). If θ is the angle of the flight path to horizontal (the glide angle),

$$L = W \cos \theta, \tag{1}$$

and

$$D = W \sin \theta. \tag{2}$$

In this study, L and W are identical since cos θ is approximately 1.

Lift and drag forces are related to non-dimensional coefficients by the equations

$$C_L = 2L/(\rho S V^2) \tag{3}$$

and

$$C_D = 2D/(\rho S V^2), \tag{4}$$

where C_L and C_D are the lift and drag coefficients respectively, S is an appropriate surface area, and V is the air speed. Air density (ρ) is 1·18 kg./m^3. in this study, and

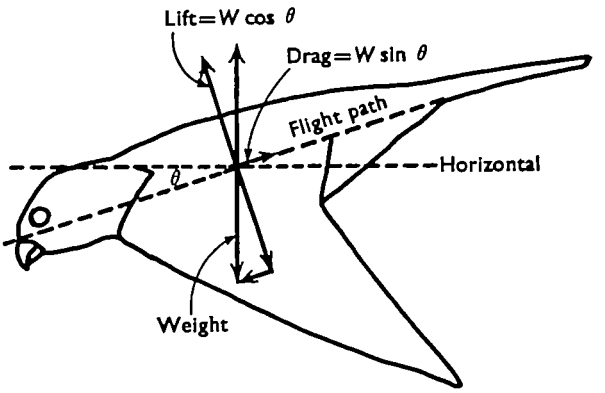

Fig. 1. Forces on a bird during equilibrium gliding. The glide path is inclined at angle θ to horizontal. The lift and drag forces act perpendicularly and parallel respectively to the glide path and are balanced by components of the weight force.

all dimensions are in the meter-kilogram-second system. Accordingly, forces are given in newtons. They may be converted into kg. by dividing by the acceleration of gravity, 9·8 m./sec.^{2}.

The value for S is usually wing area, defined as the projected area of both wings including the area intercepted by the body. Occasionally S represents the total area, or total 'wetted' area, of the bird. Henceforth, we will use S and S_w for wing area and total wetted area, respectively. The wetted area of the wings is 2·04 times their projected area. This factor takes into account both the upper and lower surfaces of the wings and their curvature.

Other aerodynamic parameters we will use are wing span (b), the distance from wing tip to wing tip; wing chord (c), the ratio of wing area to b; and aspect ratio (AR), the ratio of wing span to wing chord or b^2/S.

Reynolds number (Re) is an important part of the description of gliding per-

formance because it is functionally related to the lift and drag coefficients. Reynolds number is non-dimensional and is defined as

$$\mathrm{Re} = \rho V c/\mu, \tag{5}$$

where μ is the viscosity of air. The ratio ρ/μ in this study has the value 65,200.

MATERIALS AND METHODS

Wind tunnel

The wind tunnel was of open circuit design with a fan downstream of the test section (Fig. 2). The test section was rectangular in cross-section and was 2·3 m. long, 1·1 m. high and 1·4 m. wide. The air speed in the test section could be varied in steps by changing pulleys on the fan drive. The entire tunnel could tilt 8° about its transverse axis.

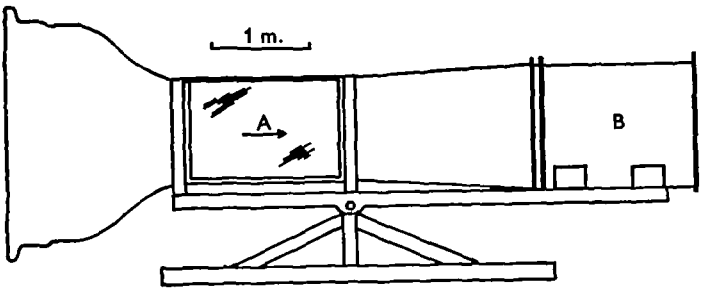

Fig. 2. Wind tunnel mounted on a pivoted frame. The bird flies in the test section (A), where an arrow shows the direction of air flow. An internal, axial fan at B draws air through the tunnel.

We have described the air flow in the test section by three quantities—speed, turbulence and direction. These quantities were measured in a three-dimensional array of 12 points in the region of the test section where the bird flew. Air speed was measured to an accuracy of 1% with a Pitot-static tube connected to a micromanometer, and within the array of points it varied ±5% from the mean value.

Turbulence was measured with a turbulence sphere and with a DISA 55D05 hot-wire anemometer connected to a true root-mean-square voltmeter. A turbulence factor was obtained by determining the Re value for the sphere as its boundary layer changed from laminar to turbulent (Pope & Harper, 1966). The hot-wire anemometer measured the percentage of turbulence, defined as

$$\%\ \text{turbulence} = 100 V_{\mathrm{rms}}/V_{\mathrm{dc}} \tag{6}$$

where V_{rms} and V_{dc} are the root-mean-square a.c. voltage and d.c. voltage outputs respectively of a linearized anemometer.

In experiments with the falcon the percentage of turbulence was between 1 and 2%. The turbulence factor in the centre of the test section was 3. Much of the turbulence was generated by a screen of hardware cloth (1·3 cm. mesh) at the upstream end of the test section. This screen was removed for experiments with the model aircraft, reducing turbulence to less than 0·5% and the turbulence factor to 1·3. We have not used the turbulence factors to calculate effective Re (Jacobs & Sherman, 1937)

because we have no information on how turbulence and Re interact to influence the aerodynamic forces produced by a feathered rather than a smooth wing.

The direction of air flow was measured with a yawmeter connected to a differential pressure transducer. This method could detect a change of direction of 0·1°. The axis of the yawmeter was lined up parallel to the air flow by the conventional method of rotating the yawmeter through 180°. The direction of air flow varied as much as 1° in the region of the test section where the bird flew. The mean value, accurate to 0·5°, has been used in all computations. This level of accuracy results in drag values that are accurate to better than 9% and does not introduce an appreciable error into the lift values.

Wind-tunnel boundary corrections (Pope & Harper, 1966) are less than 1·5% for dynamic pressure effects on lift and drag, streamline curvature effects on lift, and horizontal buoyancy effects on drag. We did not correct our data for any of these effects. However, downwash corrections for drag were as high as 13%, and unless stated otherwise we corrected our measured drag values (D_m) as follows:

$$D = D_m + \frac{\rho(SC_L V)^2}{16C}, \tag{7}$$

where C is the cross-section area of the wind-tunnel test section (1·5 m.^{2}), and the other symbols have been defined.

DIMENSIONS

The area and shape of the falcon's wings at each speed and glide angle were determined from photographs taken from directly above the bird when it was gliding at equilibrium (moving less than 0·02 m./sec. relative to the tunnel). Wing area was

Table 1. *Dimensions and references for selected aircraft*

Aircraft	Weight (newtons)	Wing span (m.)	Wing area (m.^{2})	Total wetted area (m.^{2})	Reference
Falcon *Falco jugger*	5·6	0·568 to 1·01	0·112*b* +0·019	0·228*b* +0·062	This study
Black Vulture *Coragyps atratus*	22·5	1·44	0·364	1·06	Raspet, 1950 1960
Fulmar *Fulmarus glacialis*	7·1	1·09	0·102	0·288	Pennycuick, 1960
Pigeon *Columba livia*	3·7	0·450 to 0·640	0·0491 to 0·0580	0·142 to 0·161	Pennycuick, 1968
Gull model	3·2	0·900	0·0870	0·205	Feldmann, 1944
Astro-mite model	3·2	1·12	0·158	0·639	This study
SHK sailplane	3630	17·1	14·7	46·2	Schemp–Hirth KG. 7312 Kircheim–Teck, Germany

obtained by tracing the photographs, cutting out and weighing the tracings of the wings, and multiplying their weight by a factor that corrected for scale and converted to area units. The scale factor was determined for each photograph from the width of the wing base, which remained constant on the bird at all flight speeds and angles. Wing areas are accurate to 5%.

Body-surface areas of the falcon and other birds were calculated by representing

the body as a truncated sphere (the head), a frustrum (the neck and pectoral region) and a cone (the abdomen). Appropriate dimensions were obtained from live birds or photographs. This method is accurate to about 20%.

The total wetted areas of birds were calculated by adding body area to the wetted area of the wings and tail and deducting the wing and body areas that overlap one another. (Errors in the estimate of body area are relatively unimportant since the body makes up less than one-third of total wetted area.) Wetted areas of a man-made sailplane (Schemp-Hirth, Model SHK) and a model aircraft were determined from manufacturer's figures and scale drawings. Wetted areas are accurate to 10%.

Various dimensions for some of the birds and other aircraft discussed in this study are given in Table 1.

Model aircraft

Measurements of the lift and drag forces on a model aircraft (Astro-mite, Midwest Products Co., Fig. 3) of about the same size as the falcon were made for comparative purposes. The aircraft was attached by the nose to a two-component flight balance

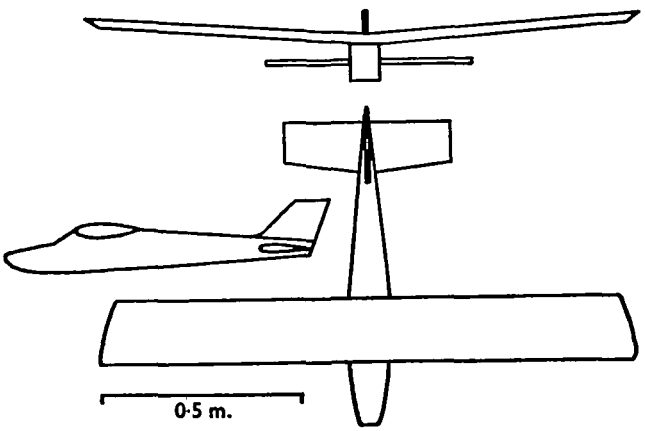

Fig. 3. Astro-mite model aircraft. Wings and horizontal stabilizer are made of solid styrofoam. All other parts are made of balsa wood.

(Fig. 4) through a pivot joint so that the aircraft was free to assume an appropriate flight attitude relative to a horizontal air stream. The horizontal stabilizer of the aircraft could be trimmed to vary the lift and drag forces at a given air speed.

The flight balance measured the vertical component of force (F) on the nose of the aircraft by transmitting it through a vertical rod on linear ball bearings to a Mettler balance beneath the wind tunnel. The angle (ϕ) of the pivoted arm of the balance was read to 0·5° relative to the horizontal air stream with a protractor. The drag of the aircraft is given by

$$D = F \cot \phi. \tag{8}$$

Lift is the sum of F and the weight of the aircraft.

The accuracy of the flight balance was determined by using weights to apply known forces to the pivoted arm at known angles. Over the range of forces and angles used in this study, the balance was accurate to better than 5%.

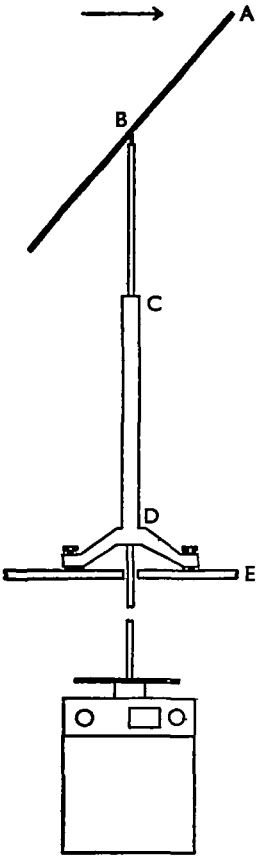

Fig. 4. Two-component flight balance. The arrow shows the direction of air flow. The model aircraft attaches by the nose to the rigid arm at A through a pivot joint. The arm is balanced for both aerodynamic and gravitational forces, and connects to the vertical rod through a pivot joint at B. The rod passes through a casing where it is supported by linear ball bearings at C and D. The rod penetrates the floor of the wind tunnel (E) and transmits the vertical force on the nose of the model to the balance. The horizontal force on the model is calculated after measuring the angle of the pivoted arm relative to horizontal. The model's performance in the wind tunnel can theoretically be duplicated in free flight simply by adding weight to the nose equivalent to the force measured by the balance.

Experimental animal and procedure

The falcon was obtained from an animal dealer. It was trained to fly in the wind tunnel by giving it mild shocks from an electrical grid on the floor of the test section. After several weeks of training, it would alternately flap and glide in the wind tunnel for a half hour or more. The falcon weighed 0·57 kg. (5·6 newtons) throughout the experiments.

The experimental procedure was to start the bird gliding at a given speed with the tunnel tilted to 8°. After a series of photographs had been taken the tunnel was tilted to 7°. The process was repeated at 1° intervals until the bird would no longer glide at equilibrium. Then the tilt of the tunnel was adjusted to the minimum angle where the bird could just glide at equilibrium. After photographs were taken, this minimum

glide angle was measured to the nearest 0·5°. The process was repeated for various speed steps until the speed became too high or low for the falcon to glide at equilibrium when the tunnel was tilted to its maximum angle of 8°.

RESULTS

The falcon typically glided at equilibrium for about 5 sec., then flapped its wings and flew forward, drifted back in a glide and again glided at equilibrium for several seconds. It responded to increases in both air speed and glide angle in the same way—by flexing its wings and decreasing wing area (Fig. 5). Both wing shape and wing area were related to wing span (Figs. 6 and 7).

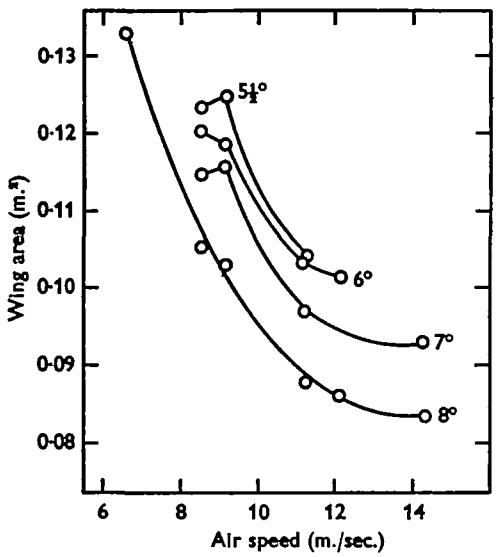

Fig. 5

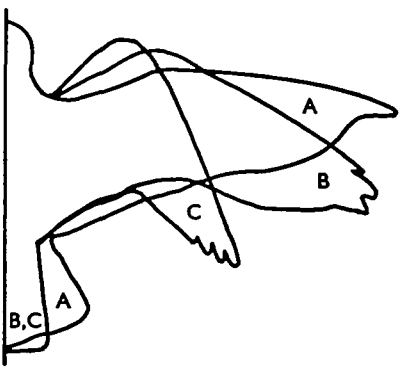

Fig. 6

Fig. 5. Mean wing area of the falcon in the wind tunnel at different speeds and glide angles. Mean sample size for each point is 5; mean standard deviation is 0·006.

Fig. 6. Wing and tail shape of the falcon at various speeds and glide angles. A, 6·6 m./sec., 6°; B, 8·5 m./sec., 5°; C, 14·3 m./sec., 6°.

The lift coefficient of the wings decreased at all glide angles as speed increased (Fig. 8). The maximum lift coefficient of 1·6 is similar to those measured in other tunnels for wings with highly cambered airfoils like that of the falcon (Table 4).

The minimum glide angle of the falcon was constant over a range of intermediate speeds and increased at higher or lower speeds (Fig. 9). Wing span and total drag at the minimum glide angles for various speeds are shown in Table 2.

For the model aircraft, polar plots of the lift and drag forces formed a family of linear curves, one for each speed (Fig. 10).

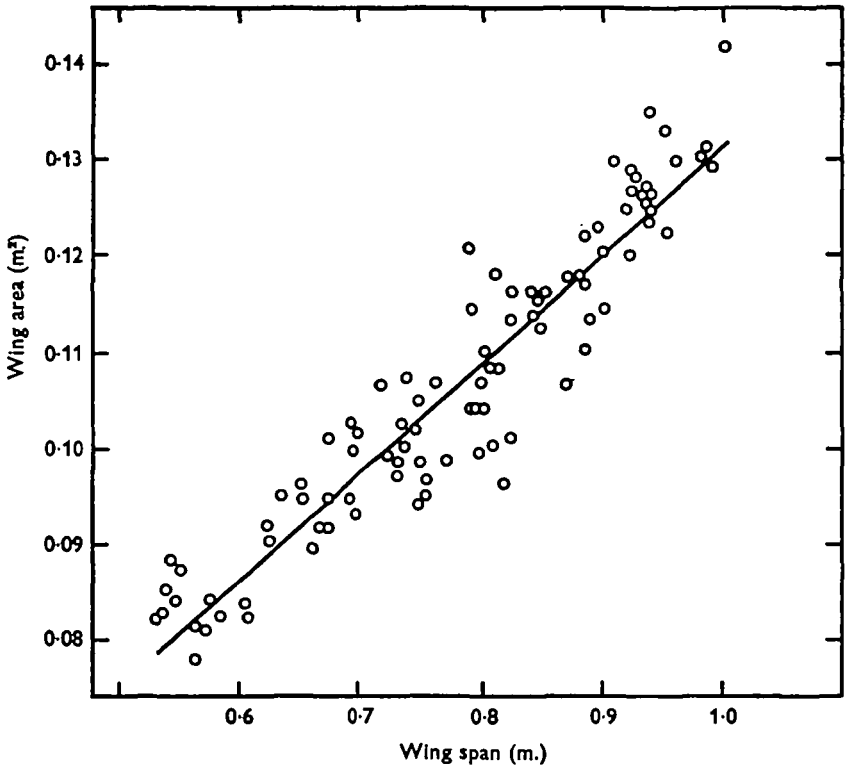

Fig. 7. Wing area of the falcon at various wing spans. The equation of the least squares regression line is $S = 0{\cdot}112b + 0{\cdot}019$ ($N = 94$, standard error of estimate = 0·0053).

DISCUSSION

Measurements of gliding performance

The basic performance of an aircraft during equilibrium gliding in still air is described by three parameters: airspeed, glide angle (θ) and sinking speed relative to the air. If any two of these parameters are known, the third can be calculated, since sinking speed is the product of airspeed and sin θ. Usually the ratio of lift force to drag force (L/D) is given rather than θ. The L/D value describes the distance travelled forward for a given loss in altitude and is equal to cot θ. For gliders, θ is usually less than 8° so that the approximation cot $\theta = 1/\sin\theta$ is accurate within 1% or better, and the equation

$$\text{sinking speed} = V/(L/D) \tag{9}$$

may be used.

The conventional way of summarizing the performance of a glider is by plotting sinking speed against air speed. In such a diagram points representing a given L/D value fall along a straight line that passes through the origin, and the complete range of air speeds, sinking speeds and L/D values for a glider can be read directly. We have used such a diagram (Fig. 11) to show the gliding performance of different birds and bird models, the model aircraft, and the full-size, high-performance sailplane.

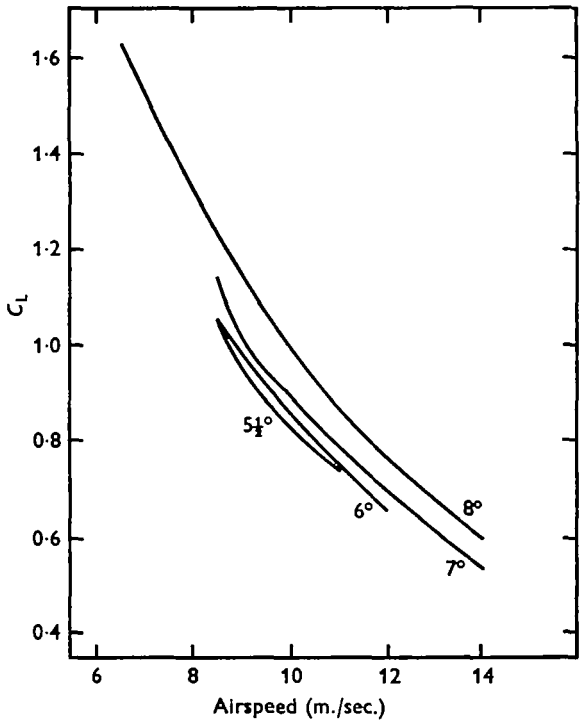

Fig. 8. Lift coefficient of the falcon at different speeds and glide angles.

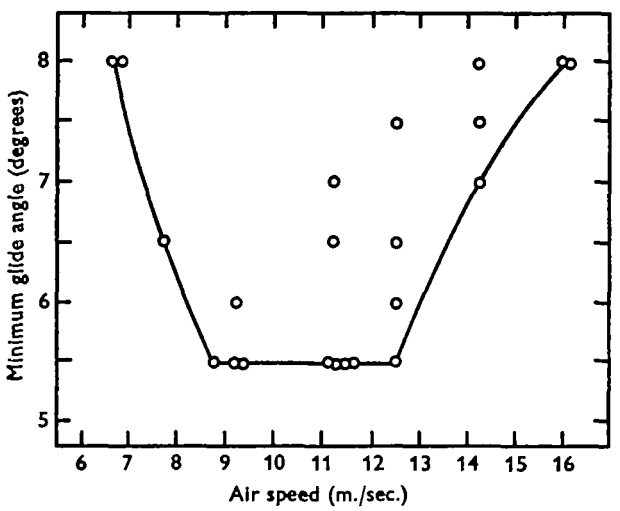

Fig. 9. Minimum glide angle of the falcon at different speeds. The curve is fitted to the lower boundary of the points.

To evaluate the performance of the various birds and other aircraft we shall consider two goals of gliding flight: covering distance over the ground toward a destination and remaining aloft by static soaring. Any particular aircraft achieves these goals to a degree determined by its aerodynamic characteristics and the atmospheric condi-

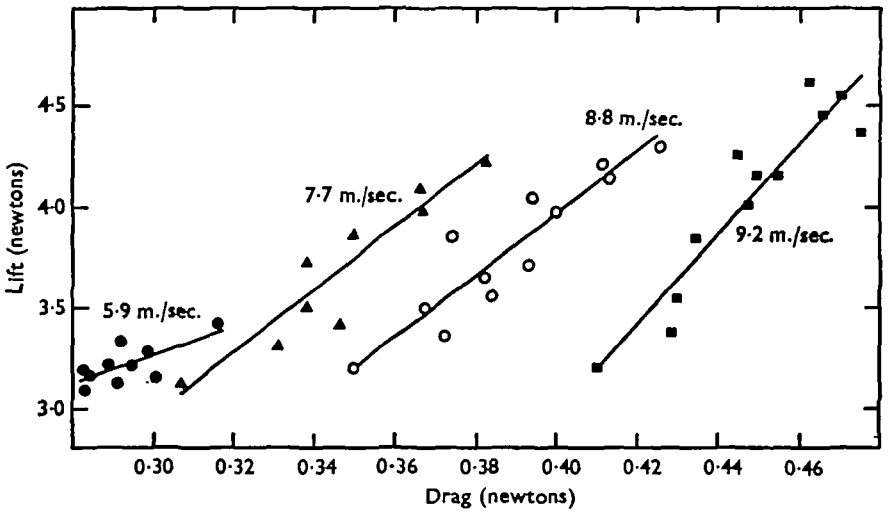

Fig. 10. Polar plot of the lift and drag forces on the Astro-mite model aircraft. The lines, fitted by least squares, have slopes, intercepts and standard errors of estimate given in order following the appropriate symbol: ●, 6·9, 1·19, 0·076; ▲, 15·5, −1·67, 0·134; ○, 15·2, −2·13, 0·142; ■, 22·4, −5·99, 0·168. These data have not been corrected for tunnel boundary effects.

Table 2. *Basic data for the falcon at minimum glide angles*

Speed (m./sec.)	Wing span (m.)	Total drag (newtons)
6·6	1·01	0·889
8·2	0·908	0·654
9·5	0·899	0·586
10·5	0·805	0·577
11·5	0·742	0·571
12·5	0·729	0·566
14·2	0·595	0·713
15·9	0·568	0·806

tions. In general the characteristics that are optimum for one goal or set of atmospheric conditions are not optimum for other conditions or for the other goal. We shall show that an aircraft with a higher L/D value than another is favoured for achieving both goals under almost all atmospheric conditions.

The distance covered over the ground (x) by a gliding aircraft from an initial altitude (h_0) depends on L/D, air speed (V) and wind velocity assuming that wind velocity has only steady, horizontal components (U) that are parallel to the plane containing the glide angle (θ)—that is, there are no updraughts, downdraughts or sidewinds. The relations between these variables are shown in the following equations and velocity vector diagram (Fig. 12), where t is the time of travel:

$$dx/dt = dh/dt \cot\theta + U = dh/dt\ L/D + U, \tag{10}$$

$$dt = dh/(V \sin\theta) = dh\ L/(DV), \tag{11}$$

$$x = h_0\,(1 + U/V)\,L/D. \tag{12}$$

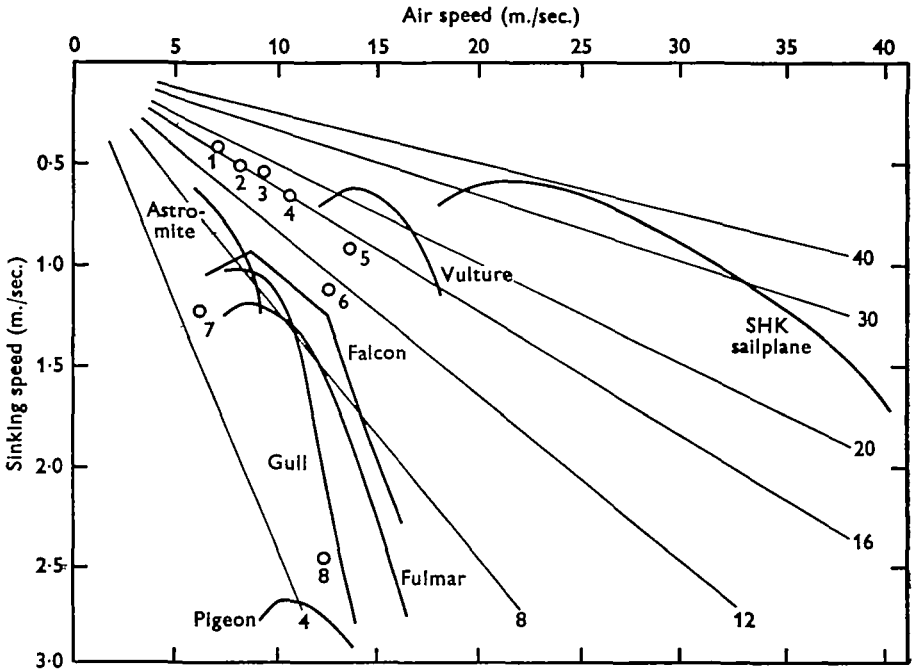

Fig. 11. Sinking speeds at minimum glide angles and various air speeds of gliding birds in nature and live, stuffed or model birds in wind tunnels. Also included are curves for the Astro-mite model and the SHK sailplane. All points on each straight, diagonal line have the same lift/drag value, which is given at the end of each line. The species and references for birds represented by curves are given in Table 1. Birds represented by numbered points are: (1) kite (Idrac, 1931); (2) vulture, *Perenoptere moine* (Idrac, 1931); (3) vulture, *Pseudogyps africanus* (Idrac, 1931); (4) vulture, *Gyps fulvus* (Idrac, 1931); (5) laughing gull, *Larus atricilla* (Raspet, 1960); (6) black vulture, *Coragyps atratus* (Parrott, 1969); (7) Alsatian swift, stuffed (Nayler & Simmons, 1921); (8) kite, stuffed (Le Page, 1923).

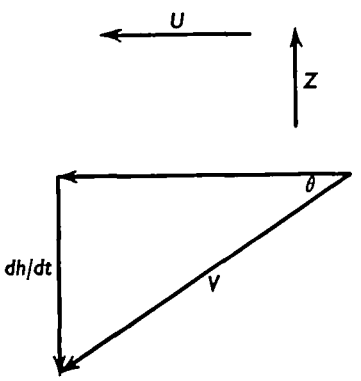

Fig. 12. Velocity vector diagram for a gliding bird showing the relations between air speed (V), glide angle (θ) and rate of change of altitude (dh/dt). The horizontal and vertical wind velocity vectors (U and Z, respectively) are also shown. All vectors except dh/dt are shown in the positive direction.

The value of x can be maximized in various atmospheric conditions by maximizing or minimizing appropriate variables of equation (12) (Table 3).

If the vertical velocity component of the wind (Z) is not zero, the aircraft may static-soar, and the increase or decrease of altitude above the ground depends on air speed, L/D, and the time of travel through the air. Thus,

$$dh = (Z - \text{sinking speed})\, dt, \tag{13}$$

$$h = [Z - V/(L/D)]t + h_0. \tag{14}$$

The value of h can be maximized for various atmospheric conditions by maximizing or minimizing appropriate variables of equation (14) (Table 3).

Table 3. *Strategies for maximizing distance travelled or altitude gained in various environmental conditions*

To maximize	Environmental conditions and equivalent mathematical description	Maximize	Minimize
	Tail wind		
Distance travelled	$1+U/V > 0$, $U > 0$	L/D	V
in positive direction (x)	Head wind, glider gaining ground		
$x = h_0(1+U/V)\, L/D$	$1+U/V > 0$, $U < 0$	L/D, V	
	Head wind, glider losing ground		
	$1+U/V < 0$, $U < 0$	V	L/D
Altitude (h)	Updraught, greater than sinking speed		
$h = [Z - V(L/D)]\, t + h_0$	$Z - V/(L/D) > 0$, $Z > 0$	L/D, t	V
	Updraught, less than sinking speed		
	$Z - V/(L/D) < 0$, $Z > 0$	L/D	V, t
	Downdraught		
	$Z - V/(L/D) < 0$, $Z < 0$	L/D	V, t

For the simplified goals and environmental conditions, described above, Table 3 shows that the higher the L/D value the better the performance except when a head-wind is strong enough to move the aircraft backwards. Then the least ground is lost by landing as quickly as possible. High air speed is an advantage only when gliding against a head wind, and a low sinking speed is beneficial except in a head wind. Prolongation of flight time, for example, by circling, benefits an aircraft in a region of air that is ascending faster than the sinking speed of the aircraft.

The maximum L/D values achieved by the aircraft in Fig. 11 vary widely, from less than 5 for the pigeon to 38 for the sailplane. However, the data are consistent with a maximum L/D value in the vicinity of 10 for soaring birds and the model aircraft. Idrac (1931) gives L/D values of 16 or 17 for various vultures and a related bird (a kite), but these values do not differ from 10 within the accuracy of his methods. Idrac used a rangefinder and angles of altitude and azimuth to record the flight paths of birds in nature. He determined the direction of air flow where a bird was flying by measuring the tension vector of a kite string, the direction of a streamer in the wind,

or the path of a hydrogen balloon. He carefully described the accuracy of these methods.

Pennycuick (1960) gives a maximum L/D value of 8·3 for the fulmar, which does not differ from 10 within the accuracy of his methods. He determined the flight paths of these birds in nature using a method similar to Idrac's. Wind speed and direction where the birds were gliding were determined with a cup anemometer and a wind vane attached to a pole.

Feldmann (1944) made lift and drag measurements on a plaster model of a gull suspended in a wind tunnel. His values give a maximum L/D value of 8·7 for a 0·33 kg. bird. A maximum L/D value of 4·6 for a stuffed kite in a wind tunnel (Le Page, 1923) undoubtedly is too low, presumably because the model did not represent a living bird.

Parrott (1969) investigated a living black vulture trained to fly in a wind tunnel. His methods were the same as described for this paper. He found a maximum L/D value of 11·6.

Raspet (1950, 1960) reports maximum L/D values of 15 and 23, respectively, for the laughing gull and the black vulture. Raspet used a sailplane of known performance to follow soaring birds. He calculated gliding performance from the air speed of the sailplane and the position of the birds relative to it. Raspet does not evaluate the accuracy of this method, but mentions that errors could be introduced if the birds soar on air currents that the sailplane does not utilize. We believe that such errors are responsible for Raspet's high values of L/D (see discussion in section on *Estimation of drag*).

The falcon has a maximum L/D value of 10. The model aircraft also has a maximum L/D value of 10, and Schmitz (1952) gives this value for other model aircraft of similar size.

Because of their much lower L/D values compared to the sailplane, soaring birds have inferior performance when their goal is covering distance over the ground in still air or against a head wind. However, performance under these conditions is probably less important to a bird than it is to a sailplane pilot, who risks destruction if he cannot land at an airfield. Soaring birds are powered aircraft as well as gliders and have folding wings and landing gear that enable them to land and take off almost anywhere.

When the goal is static-soaring, the birds are comparable to or better than the sailplane. Static-soaring ability depends on both L/D and V in such a manner that it improves when the ratio $V/(L/D)$, or sinking speed, is low (Table 3). The birds have comparable sinking speeds to the sailplane because their low flight speeds and low L/D values compensate one another (Fig. 11). In fact, sailplane pilots commonly report that birds can soar when sailplanes cannot, or that soaring birds gain altitude faster than sailplanes in regions of ascending air. The birds may have lower sinking speeds than the sailplane, or because of their lower speed, smaller size and superior manoeuvrability they may be able to remain in regions of ascending air that are too small to contain the sailplane.

Estimation of gliding performance

In this section we present a method of estimating the equilibrium gliding performance of a bird in the absence of wind tunnel tests. We have shown how gliding

performance is determined by air speed, lift and drag. Air speed can be measured in nature, and lift is simply the weight of the bird. The problem is to estimate the drag force. The following discussion summarizes aerodynamic relations that can be used to make estimates of drag. Additional details can be found in Goldstein (1965), Jones (1950), Perkins & Hage (1950), Prandtl & Tietjens (1957), Schmitz (1952) and von Mises (1959).

Induced drag. The total drag of an aircraft is the sum of two components—induced drag and parasite drag. Induced drag is associated entirely with the production of lift. Prandtl's wing theory and a large body of experimental evidence indicate that the induced drag coefficient of wings is given by the relation

$$C_{Di} = C_L^2/(\pi M^2 AR), \tag{15}$$

and that the induced drag is given by the relation

$$Di = 2L^2/(\pi\rho M^2 V^2 b^2). \tag{16}$$

The value of the factor M (Munk's span factor; von Mises, 1959) depends on the distribution of lift along the wing span. It has a maximum of 1, both in theory and practice, for wings with an elliptical lift distribution. However, the value of M^2 changes relatively little with lift distribution and usually is between 0·9 and 0·95 for airplane wings. We will use a value of 0·9 for M^2 to calculate the induced drag of birds.

Parasite drag. Parasite drag is produced by pressure differences and skin friction. The laminar or turbulent condition of the boundary layer can have large effects on both of these. Skin friction drag is minimal when the boundary layer is laminar and increases markedly when the boundary layer goes through transition and becomes turbulent. On the other hand, parasite drag may decrease with transition. This is because transition may allow air flow to follow the contours of a curved object more closely, thereby reducing pressure drag more than enough to compensate for the increase in skin friction.

The opposite effects of transition on skin friction and pressure drag can lead to confusion. For example, a 'laminar flow airfoil' has both a lower parasite drag than a conventional airfoil and a more extensive laminar boundary layer. The airfoil has, therefore, low skin-friction drag but also has low pressure drag because it is shaped in such a way that transition occurs in the appropriate region to allow air flow to follow the curvature of the airfoil. In contrast, conventional airfoils and airfoils shaped like those found in bird wings have less parasite drag when the boundary layer is largely turbulent rather than laminar. In this condition the increase in skin friction with turbulence is more than compensated for by the reduction of pressure drag.

The laminar or turbulent condition of the boundary layer is related to the roughness and shape of the surface, the turbulence of the air before it passes over the surface and the Re value for the surface. The soaring birds under discussion here fly at Re values in the region where transition from a laminar to a turbulent boundary layer takes place in conventional airfoils (Schmitz, 1952). Since transition can increase the L/D value for a wing by a factor of 2 or more (Schmitz, 1952), the condition of the boundary layer can have a profound effect on gliding performance. Model air-

planes and golf balls also operate at Re values where transition may occur. Model builders sometimes roughen the wings of their models to induce turbulence (Pearce, 1961), and golf ball manufacturers make dimples on their product for the same reason.

Equivalent parasite area. The parasite drag of an aircraft may be calculated in the absence of wind-tunnel tests by estimating an 'equivalent parasite area' (f) (Perkins & Hage, 1950). This area may be thought of as the wetted area of a hypothetical object with the same parasite drag as the total aircraft, but with a parasite-drag coefficient (C_{Dp}) arbitrarily assigned a value of 1. Thus,

$$\tfrac{1}{2}\rho C_{Dp1} f V^2 = \tfrac{1}{2}\rho C_{Dp2} S_w V^2, \tag{17}$$

where C_{Dp1} is the parasite-drag coefficient (equal to 1) of the hypothetical object, C_{Dp2} is the parasite-drag coefficient of the aircraft and S_w is the wetted area of the aircraft. The value of C_{Dp2} is estimated from measurements made on an existing aircraft similar to the one under investigation.

A modification of this method may be used for estimating the parasite drag of birds. The modification lies in assigning to C_{Dp1} the value of the parasite drag coefficien (C_f) of a smooth, flat plate oriented parallel to the direction of air flow and with turbulent boundary layer. Values of C_f at various Re values have been thoroughl investigated and can be calculated from Prandtl's formula (Goldstein, 1965)

$$C_f = 0{\cdot}455(\log_{10} \mathrm{Re})^{-2{\cdot}58}. \tag{18}$$

Values of Re are calculated for the chord of the aircraft's wing and the chord of th flat plate. Substituting C_f for C_{Dp1} in equation (17), and cancelling and re-arranging gives

$$S_w C_{Dp}/C_f = K S_w = f, \tag{19}$$

where f now is the wetted area of a flat parallel plate with the same drag as the bird under investigation. The factor K is simply the ratio of the parasite-drag coefficient of the bird (C_{Dp}) to that of the plate at the appropriate Re value. If K is estimated from information on other birds, C_{Dp} for the bird under investigation may be calculated.

The advantage of making C_{Dp1} of equation (17) a variable rather than assigning it a value of 1 is that this modification allows for the variation of parasite drag with Re and permits comparison of different aircraft over a wide range of Re. This consideration is important to an investigation of the aerodynamic characteristics of birds, which fly at Re values where little aerodynamic information exists.

Estimation of drag. To determine K values for birds we have collected all the relevant information that we could find on parasite-drag coefficients (Fig. 13). This figure includes data for birds at minimum glide angles, the model aircraft, the high-performance sailplane, wings with various airfoils and flat plates. The airfoils for the aircraft and wings are described in Fig. 14 and Table 4.

At maximum L/D, K values for birds (excluding Raspet's black vulture) range from 2·2 for Parrott's black vulture to 4·3 for the pigeon (Table 5). The model aircraft, while similar in size to the birds, is aerodynamically cleaner, with a K at maximum L/D of 1·8.

Although the birds are not nearly as aerodynamically clean as the sailplane (K value, 0·7), they do about as well as some propeller-driven aircraft. Data from Perkins & Hage (1950) for various World War II military airplanes yield K values of 1·3 to 5·0 at an Re of 10^7.

Wings with airfoils similar to those of the aircraft in Fig. 13 have K values between 0·5 and 7. In many cases, C_{Dp} values for these wings are close to those for the appropriate aircraft. This is not surprising, for the wetted area of the wings comprises 50 to 90% of the total wetted area. Thus the sailplane has a K of less than 1 because it uses a laminar flow Eppler 266 airfoil similar to the NACA airfoils in Fig. 14.

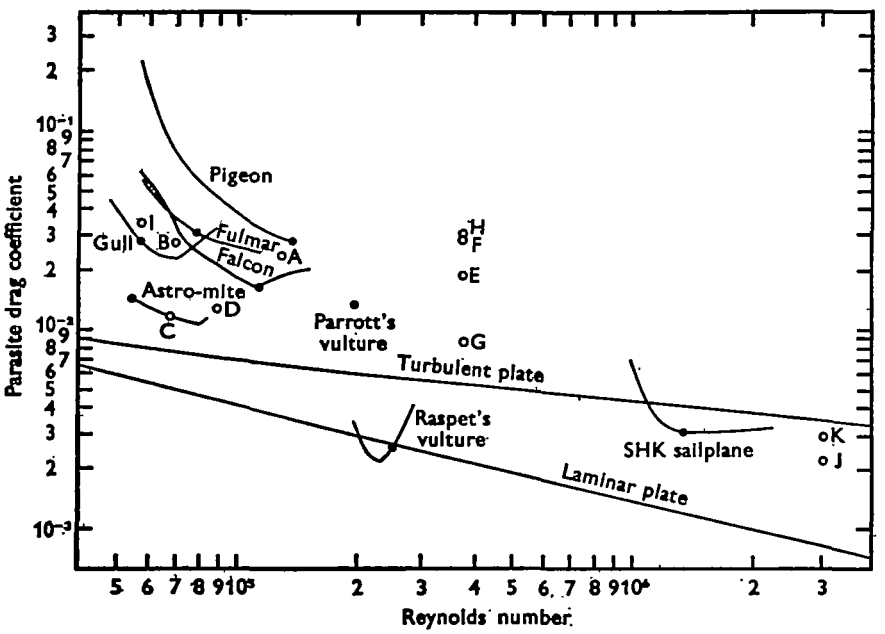

Fig. 13. Parasite-drag coefficients at different Reynolds numbers for various birds at minimum glide angles, the Astro-mite model, the SHK sailplane, wings with different airfoils (open circles) and flat plates. The solid circle on each curve marks the parasite-drag coefficient at the maximum L/D value. The upper diagonal line for a flat parallel plate with a turbulent boundary layer is calculated from Prandtl's formula. The lower diagonal line for a flat parallel plate with a laminar boundary layer is calculated from the formula of Blasius, $C_f = 1{\cdot}328\ \mathrm{Re}^{-0{\cdot}5}$. The parasite-drag coefficients for wings are identified by airfoil letters and are based on wetted area. Thus, they are equal to the minimum drag coefficient divided by 2·04. The airfoils are described in Fig. 14 and Table 4.

Values for parasite-drag coefficients calculated from Raspet's data for the vulture are very different from those for other birds. They fall entirely below the line for a flat plate with a turbulent boundary layer, and some fall as much as 19% below the laminar flat plate line, which is described by the formula of Blasius (Goldstein, 1965).

Raspet (1950, 1960) suggests that the low parasite-drag coefficients for the vulture may result from some form of boundary layer control, perhaps due to the porosity of feathers, that keeps the boundary layer laminar. Even if this were the case, it is difficult to imagine how the vulture could have lower C_{Dp} values than a flat, parallel plate with a laminar boundary layer. On such a plate there are no pressure differences

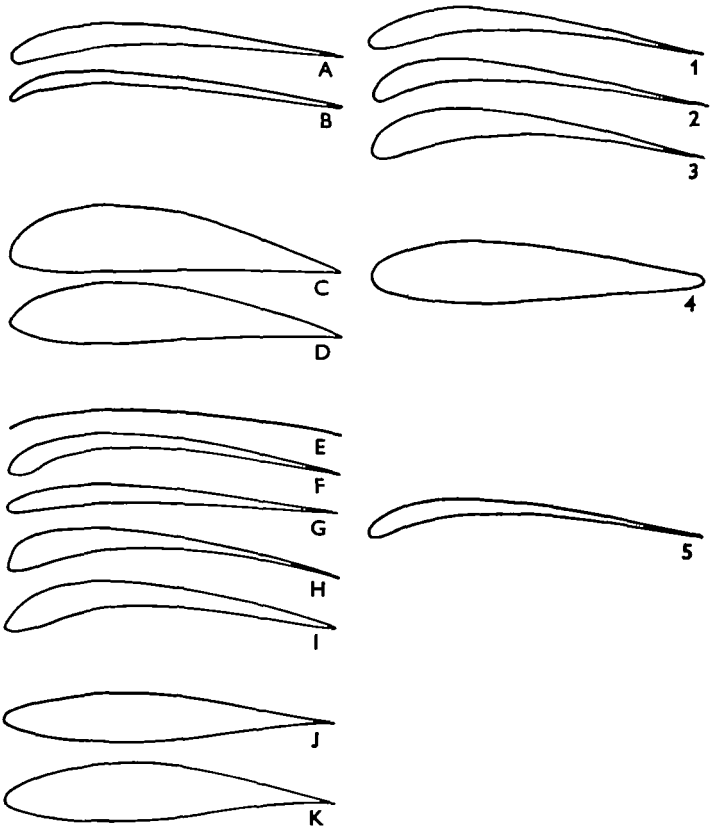

Fig. 14. Tested airfoils (left, lettered) and similar airfoils (right, numbered) used on the aircraft described in Fig. 13. Data for the tested airfoils also appear in Fig. 13. Airfoils with similar shapes and Reynolds numbers are grouped together, and are identified in Table 4. (Airfoil I has been inadvertantly misplaced. It belongs with A and B).

Table 4. *Identification and aerodynamic characteristics of airfoils* (*Fig.* 14)

Airfoil	Maximum C_L	Minimum C_D	Re × 10^{-6}	Reference
A. Eiffel 13	1·2	0·050	0·34	NACA TR no. 93
B. Göttingen 265	1·6	0·054	0·67	NACA TR no. 124
C. Göttingen 290	1·0	0·024	0·67	NACA TR no. 124
D. Göttingen 255	1·4	0·026	0·90	NACA TR no. 124
E. Göttingen 417a	1·3	0·038	3·76	NACA TR no. 286
F. Göttingen 464	1·6	0·059	3·76	NACA TR no. 286
G. Göttingen 400	1·1	0·018	3·76	NACA TR no. 124
H. Göttingen 461	1·6	0·063	3·78	NACA TR no. 182
I. RAF 19	1·7	0·072	0·58	NACA TR no. 93
J. NACA 64_2215	1·4	0·0053	30	Abbott & Doenhoff, 1959
K. NACA 64_3618	1·4	0·0058	30	Abbott & Doenhoff, 1959
1. Gull, *Larus*				Herzog, 1968
2. Falcon, *Falco*				Herzog, 1968
3. Pigeon, *Columba*				Herzog, 1968
4. Astro-mite model				This study
5. Eagle, *Aquila*				Herzog, 1968

to cause drag, and skin friction theoretically is minimum. In fact, transition from laminar to turbulent boundary layers results in a decrease, not an increase, in C_{Dp} at a given lift coefficient for the airfoils and Re values under consideration here (Schmitz, 1952). Furthermore, wind-tunnel tests on a living vulture and on wings with bird-like airfoils do not support the low C_{Dp} values calculated from Raspet's data. We feel that Raspet's values are probably explained by the possible error in technique that he mentions rather than by unconventional aerodynamics.

Table 5. *K values at maximum L/D for aircraft of Fig.* 13

Aircraft[1]	K
Falcon	2·4
Vulture[2]	2·2
Vulture[3]	0·4
Gull	3·5
Fulmar	4·1
Pigeon	4·3
Astro-mite model	1·8
SHK sailplane	0·7

1. For reference see footnote or Table 1. 2. Parrott, 1969. 3. Raspet, 1950, 1960.

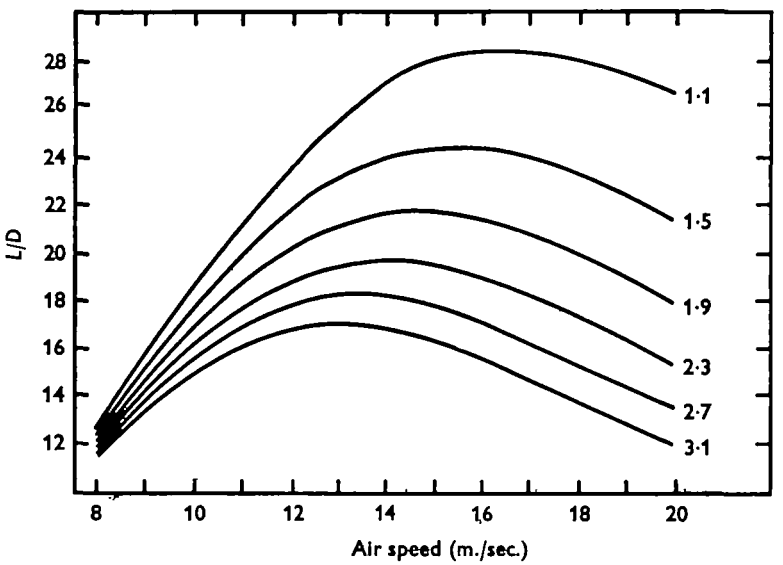

Fig. 15. Dependence of L/D value estimates for an albatross on estimated air speed and a range of possible K values. The K values are shown at the right of each curve.

As an example of how K can be used to estimate drag we have calculated the maximum L/D value for one of the largest soaring birds, the wandering albatross (*Diomedea exulans*). Appropriate data for this bird (Herzog, 1968; Jameson, 1958) are: weight = 96 newtons, wing span = 3·45 m., wing chord = 0·21 m., total wetted area = 1·55 m.^{2}, air speed = 16 m./sec. These data and equation (16) yield an induced drag of 1·8 newtons. Since the albatross looks aerodynamically clean, we will use a K value of 2·2, the lowest measured for a bird (the black vulture). This K value corresponds

to a C_{Dp} value of 0·0132 at Re = $2{\cdot}2 \times 10^5$. Thus, the parasite drag is 3·0 newtons, and total drag is 4·8 newtons. These calculations are summarized by the equations:

$$\text{Total drag} = \text{induced drag} + \text{parasite drag}, \tag{20}$$

or

$$D_T = \frac{2L^2}{\pi\rho(MVb)^2} + \frac{\rho C_{Dp} S_w V^2}{2}, \tag{21}$$

where $C_{Dp} = KC_f$. The estimate of maximum L/D is 20. The effects on the L/D estimate of various choices for air speed and K for the albatross are shown in Fig. 15. The maxima in these curves are explained in the next section.

The above calculations can be simplified by assigning values to the constants in equations (18) and (21) and making appropriate substitutions. Thus, one can estimate L/D values for birds in general knowing only air speed, K, wing area, wing span and body weight, as follows:

$$C_{Dp} = 0{\cdot}455K[\log_{10}(65{,}200VS/b)]^{-2{\cdot}58}. \tag{22}$$

Then

$$L/D = \frac{1{\cdot}67WV^2b^2}{W^2 + 2{\cdot}48C_{Dp}Sb^2V^4}. \tag{23}$$

The constants in these equations reflect the assumptions that M^2 is 0·9, the density of air is 1·18 kg./m.^{3}, and total wetted area = $2{\cdot}5S$.

Design of variable wing span aircraft

An aircraft achieves its lowest possible drag, and hence its maximum L/D value, at an air speed that depends on both induced drag and parasite drag. The former decreases as air speed increases, and the latter increases, as shown in equation (21). This equation indicates that total drag is high at both low and high speeds with a minimum at the intermediate speed where induced and parasite drag are equal. The speed for minimum drag is found by setting the derivative of total drag with respect to V equal to zero to obtain

$$V = \left(\frac{4L^2}{\pi C_{Dp} S_w (\rho Mb)^2}\right)^{\frac{1}{4}} \tag{24}$$

If an aircraft is to have the maximum possible L/D value for a given C_{Dp}, it must have a weight, wing span and wetted area that allow it to fly at the speed given by equation (24).

As an example, we have used equation (21) to calculate L/D values for the SHK sailplane at different air speeds and K values (Fig. 16). To obtain these curves we plotted points representing L/D values at different speeds and calculated K for each speed. Then we held each K value constant and varied air speed in equation (21) to obtain one curve for each plotted point.

The SHK sailplane is well designed, for it has its lowest K value at the corresponding speed given by equation (24) and thus achieves the maximum L/D value for that K. However, at higher and lower speeds, it cannot attain the maximum L/D value for a particular K value because it cannot adjust wing span or wetted area in flight.

In contrast, the falcon over its entire speed range flies closer to the speeds where

L/D is maximum for the observed wing span, wetted area and K values (Fig. 17). It accomplishes this by adjusting wing span and wetted area as speed changes. Thus, as air speed increases, the falcon decreases wing span and wetted area so that the speed given by equation (24) for maximum L/D also increases.

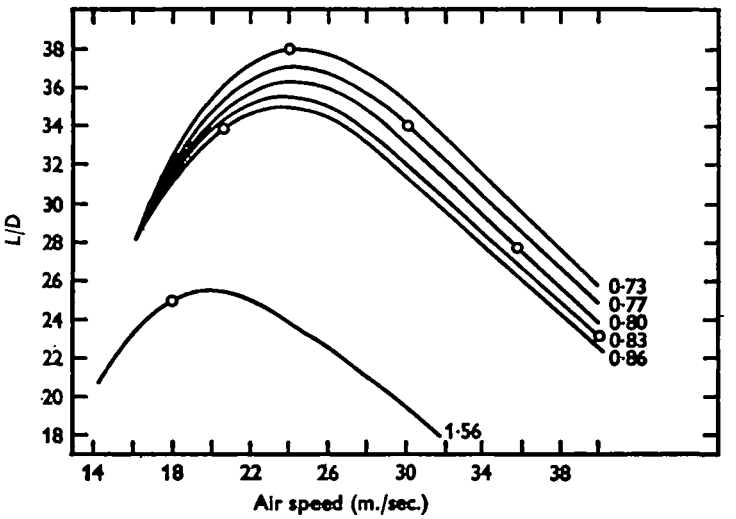

Fig. 16. Curves of possible L/D values at various speeds calculated for the SHK sailplane at different K values. The circles indicate the actual L/D values attained by the sailplane.

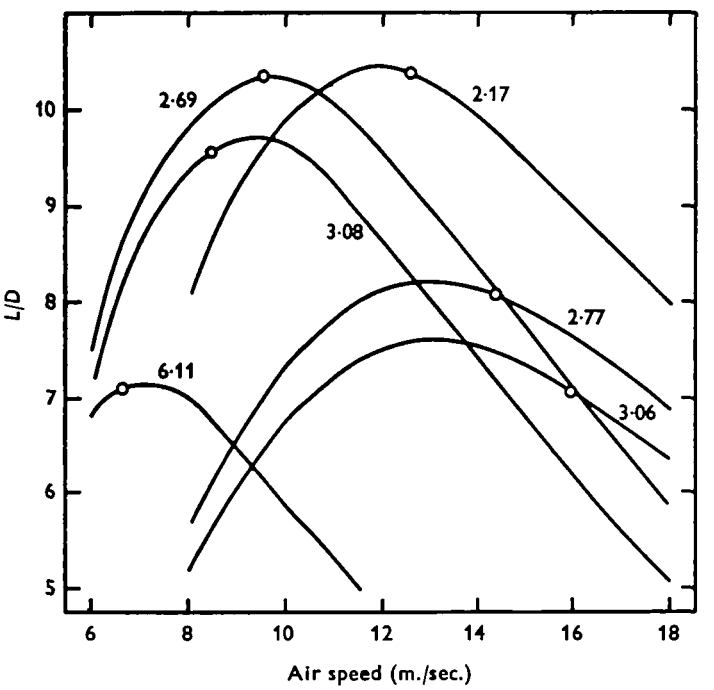

Fig. 17. Curves of possible L/D values at various speeds for the falcon at different K values. The circles indicate the actual L/D values attained by the falcon in the wind tunnel. Each K value is adjacent to the corresponding curve.

Although we have shown that the falcon at different speeds has nearly the maximum L/D value for its observed wing span, wetted area and K value, the question arises whether it could attain still greater L/D values by adjusting its wings to some other span. In other words, could the falcon in the wind tunnel increase its L/D value at a particular speed by changing its wing span to that used at some other speed? We investigated this question by determining the wing span that yields the lowest total

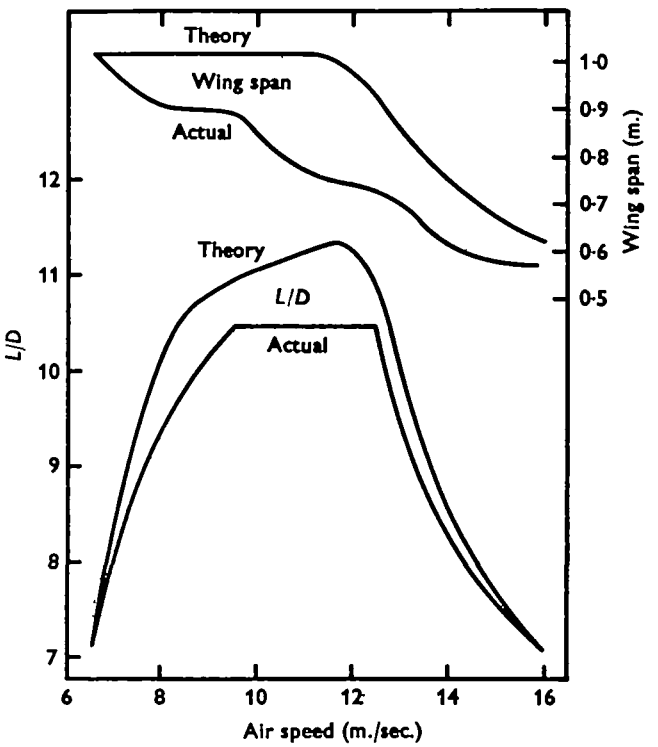

Fig. 18. Actual and theoretical wing spans and L/D values for the falcon at different speeds. If the falcon maintained the wing spans shown by the upper span curve, it could attain the L/D values shown in the upper L/D curve. In the wind tunnel the falcon actually has the wing spans and L/D values shown in the lower curves of each pair.

drag at a particular speed and C_{Dp} value. The wing span for minimum drag can be found by setting the derivative of total drag (from equation (21)) with respect to b equal to zero. Since the total wetted area of the falcon is a function of wing span

$$S_w = 0{\cdot}228b + 0{\cdot}062, \tag{25}$$

the span that minimizes drag is given by

$$b = \left(\frac{35L^2}{\pi\rho^2 M^2 C_{Dp} V^4}\right)^{\frac{1}{4}}. \tag{26}$$

We calculated the maximum L/D values for the falcon using the span values from equation (26), the observed K values at various speeds and equation (21) (Fig. 18). The falcon flies in the wind tunnel with nearly the optimum wing span and L/D over most of its speed range. The observed L/D values are close to the theoretical maximum, the largest difference being 6%.

In summary, this discussion shows that the falcon has certain features of a well-designed aircraft. For the values of wing span, wetted area and K that the falcon assumes, it achieves nearly the maximum possible L/D values. However, it could achieve slightly higher L/D values at intermediate flight speeds by extending its wings more than we observed in the wind tunnel.

Terminal speed

Falcons often kill their prey in the air by striking from a steep dive. Our measurements allow us to estimate the terminal speed of a falcon in a vertical dive. Under these conditions, total drag equals the bird's weight, and both lift and induced drag are zero. Thus, at terminal speed

$$V = \left(\frac{2W}{\rho S_w C_{Dp}}\right)^{\frac{1}{2}}. \tag{27}$$

If C_{Dp} and S_w have the minimum values we measured in the wind tunnel (0·0165 and 0·187 m.^{2}, respectively), the terminal speed is 55 m./sec. or 120 miles per hour. At this speed the falcon's wings would be partly extended with a span of 0·55 m. If we assume that the wings are completely retracted (total wetted area = 0·054 m.^{2}), the terminal speed is 100 m./sec. or 220 m.p.h. These values are consistent with the speed of a diving peregrine falcon in nature, which was estimated by an airplane pilot to be over 80 m./sec. (Lawson, 1930).

SUMMARY

1. A live laggar falcon (*Falco jugger*) glided in a wind tunnel at speeds between 6·6 and 15·9 m./sec. The bird had a maximum lift to drag ratio (L/D) of 10 at a speed of 12·5 m./sec. As the falcon increased its air speed at a given glide angle, it reduced its wing span, wing area and lift coefficient.

2. A model aircraft with about the same wingspan as the falcon had a maximum L/D value of 10.

3. Published measurements of the aerodynamic characteristics of gliding birds are summarized by presenting them in a diagram showing air speed, sinking speed and L/D values. Data for a high-performance sailplane are included. The soaring birds had maximum L/D values near 10, or about one quarter that of the sailplane. The birds glided more slowly than the sailplane and had about the same sinking speed.

4. The 'equivalent parasite area' method used by aircraft designers to estimate parasite drag was modified for use with gliding birds, and empirical data are presented to provide a means of predicting the gliding performance of a bird in the absence of wind-tunnel tests.

5. The birds in this study had conventional values for parasite drag. Technical errors seem responsible for published claims of unusually low parasite drag values in a vulture.

6. The falcon adjusted its wing span in flight to achieve nearly the maximum possible L/D value over its range of gliding speeds.

7. The maximum terminal speed of the falcon in a vertical dive is estimated to be 100 m./sec.

This study was supported by a National Science Foundation Grant (No. GB6160X), a Duke University Biomedical Sciences Support Grant (No. 303-3215) and a National Institutes of Health Training Grant (No. HE 05219). Mrs Marsha Poirier provided skilful technical assistance and computer programs.

REFERENCES

ABBOTT, I. H. & DOENHOFF, A. E. VON (1959). *Theory of Wing Sections.* New York: Dover Publ.
BEEBE, F. L. & WEBSTER, H. M. (1964). *North American Falconry and Hunting Hawks.* Denver: North American Falconry and Hunting Hawks.
FELDMANN, I. F. (1944). Windkanaluntersuchung am Modell einer Möwe. *Aero-revue,* Zurich **19**, 219–22.
GOLDSTEIN, S. (1965). *Modern Developments in Fluid Dynamics.* New York: Dover Publ.
HERZOG, K. (1968). *Anatomie und Flugbiologie der Vögel.* Stuttgart: Gustav Fischer Verlag.
IDRAC, P. (1931). *Études Expérimentales sur le Vol à Voile.* Paris: Librairie des Sciences Aéronautiques.
JACOBS, E. N. & SHERMAN, A. (1937). Airfoil Section Characteristics as Affected by Variation of the Reynolds Number. *Nat. Advisory Comm. Aeron., Tech. Rept.* no. 586, **23**, 227.
JAMESON, W. (1958). *The Wandering Albatross.* London: Rupert Hart-Davis.
JONES, B. (1950). *Elements of Practical Aerodynamics.* New York: Wiley and Sons.
LAWSON, R. (1930). The stoop of a hawk. *Bull. Essex County Orn. Club* 1930, 79–80.
LE PAGE, W. L. (1923). Wind channel experiments on a pariah kite. *Royal Aeron. Soc. London* **27**, 114–15.
MISES, R. VON (1959). *Theory of Flight.* New York: Dover Publ.
NAT. ADVISORY COMM. AERON. (1920). *Tech. Rept.* no. 93, 257–336.
NAT. ADVISORY COMM. AERON. (1921). *Tech. Rept.* no. 124, 421–74.
NAT. ADVISORY COMM. AERON. (1923). *Tech. Rept.* no. 182, 395–438.
NAT. ADVISORY COMM. AERON. (1928). *Tech. Rept.* no. 286, 139–83.
NAYLER, J. L. & SIMMONS, L. F. G. (1921). A note relating to experiments in a wind channel with an Alsatian swift. *Aeron. Res. Comm. Reports and Memoranda,* no. 708.
PARROTT, G. C. (1969). In preparation.
PEARCE, F. (1961). Airfoil turbulators. *In* Zaic, F. (ed.), *Model Aeronautic Yearbook.* New York: Model Aeronautic Publ.
PENNYCUICK, C. J. (1960). Gliding flight of the fulmar petrel. *J. exp. Biol.* **37**, 330–8.
PENNYCUICK, C. J. (1968). A wind-tunnel study of gliding flight in the pigeon *Columba livia*. *J. exp. Biol.* **49**, 509–26.
PERKINS, C. D. & HAGE, R. E. (1950). *Airplane performance stability and Control.* New York: Wiley and Sons.
POPE, A. & HARPER, J. J. (1966). *Low-speed Wind Tunnel Testing.* New York: Wiley and Sons.
PRANDTL, L. & TIETJENS, O. G. (1957). *Applied Hydro- and Aero-mechanics.* New York: Dover Publ.
RASPET, A. (1950). Performance measurements of a soaring bird. *Aeron. Engin. Rev.* **9**, 14–17.
RASPET, A. (1960). Biophysics of bird flight. *Science* **132**, 191–200.
SCHMITZ, F. W. (1952). *Aerodynamik des Flugmodells.* Duisburg: Carl Lange Verlag.